ORIGINAL ARTICLE

WILEY ORAL DISEASES

A novel 4q25 microdeletion encompassing *PITX2* associated with Rieger syndrome

Yi Yang* | Xin Wang* | Yuming Zhao | Man Qin

Department of Pediatric Dentistry, Peking University School and Hospital of Stomatology, Beijing, China

Correspondence
Man Qin, Department of Pediatric Dentistry, School and Hospital of Stomatology, 22 Zhongguancun South Avenue, Haidian District, Beijing 100081, China.
Email: qin-man@foxmail.com

Abstract

Objective: Rieger syndrome (RS) is a genetic disorder characterized by abnormal development of the eyes, teeth, and umbilicus, and the *paired-like homeodomain 2* (*PITX2*) gene is often implicated in its pathogenesis. This study aimed to identify the underlying genetic defect in a Chinese patient with RS.

Subjects and Methods: DNA samples were screened for *PITX2* gene mutations and copy number variations (CNVs) using Sanger sequencing and genomic quantitative PCR analysis (qPCR). Chromosomal microarray analysis (CMA) was performed to fine-map the CNVs.

Results: The proband suffered from severe hypodontia and conical teeth in her permanent dentition. No *PITX2* point mutations were found in this Chinese family, but a heterozygous deletion involving *PITX2* was suspected and verified by the SNPs analysis and qPCR in the proband. An approximately 0.47 Mb (chr4: 111, 334, 313–111, 799, 327, GRCh37/hg19) deletion including *PITX2* was finally determined by CMA.

Conclusions: To our knowledge, this is the first reported case of RS caused by a CNV of the *PITX2* gene in a Chinese patient. CNV screening must be considered if point mutation screens yield negative results in these patients. The distribution of SNP genotypes among family members may also provide clues about gene deletion.

KEYWORDS
Axenfeld–Rieger syndrome, eye manifestations, genetic disease, hypodontia, microdeletion, transcription factor

1 | INTRODUCTION

Axenfeld–Rieger syndrome (ARS) is a rare autosomal dominant disorder with a 1:2,000,000 prevalence (Li et al., 2014). It is mainly characterized by specific abnormalities in the anterior segment of the eye, with or without systemic manifestations (Seifi & Walter, 2017); classically, ARS is categorized as Axenfeld anomaly (AA), Axenfeld syndrome (AS), Rieger anomaly (RA), and Rieger syndrome (RS) (St et al., 2000), among which RS (OMIM 180500) is the most severe, presenting both ocular aspects and a wide variety of dental, umbilical, and craniofacial abnormalities (Engenheiro et al., 2007).

Hypodontia, microdontia, conical teeth, hypoplasia of the enamel, taurodontism, and hyperplastic maxillary labial frenum have been detected in some patients with RS (Dressler et al., 2010; Waldron, McNamara, Hewson, & McNamara, 2010). Further, midface hypoplasia, relative mandibular prognathism, a broad flat nasal root, prominent forehead, and a protruding lower lip or recessive upper lip have also been reported (Childers & Wright, 1986; Dressler et al., 2010; Lines et al., 2004).

Axenfeld–Rieger syndrome shows genetic heterogeneity and has been shown to be caused by mutations in two genes—paired-like homeodomain 2 (*PITX2*) at 4q25 and forkhead box C1 (*FOXC1*) at 6p25

*These authors contributed equally to this work.

(Hjalt & Semina, 2005). Linkage analyses have supported the involvement of a third locus, namely 13q14, but no disease-causing gene has been identified in this case (Phillips et al., 1996). Moreover, *PRDM5* and *CYP1B1* were reported to be associated with ARS in two sporadic cases (Cella et al., 2006; Micheal et al., 2016). In general, *PITX2* mutations are associated with ocular, dental, and umbilical anomalies, whereas *FOXC1* mutations are associated with isolated ocular or ocular, heart, and/or hearing defects (Tumer & Bach-Holm, 2009). A previous study found that 21 of 27 (78%) patients with ARS had dental and/or umbilical defects, and all 18 (100%) probands with ARS who presented dental and umbilical defects had *PITX2* disruptions (mutations and copy number variations [CNVs]) (Reis et al., 2012).

The *PITX2* gene encodes a developmental transcription factor that regulates the expression of downstream target genes. This protein binds to specific DNA sequences and activates transcription, whereby it plays an important role in normal embryonic development. Thus, it regulates the expression of downstream target genes (Liu, Selever, Lu, & Martin, 2003). The organs in which this gene is functional include the anterior chamber of the eye, facial bones, teeth, periumbilical skin, and cardiovascular system. The correct expression of PITX2 is fundamental for the development of these organs (Liu et al., 2003), and mutations or CNVs of *PITX2* could cause ARS.

In this study, we reported the case of a patient with RS who harbored a deletion of a region including *PITX2*. This anomaly was detected using real-time quantitative polymerase chain reaction (qPCR), and the size of the deletion was determined using chromosomal microarray analysis (CMA). Furthermore, we introduced a new and practical way to prescreen gene deletion through single nucleotide polymorphism (SNP) analysis.

2 | MATERIALS AND METHODS

2.1 | Study participants

The proband in our study was of Chinese pedigree and was clinically diagnosed with RS by an ophthalmologist. She underwent clinical and radiographic examinations, and 4 ml of peripheral blood was drawn for analysis. Routine G-band cytogenetic analysis conducted at another hospital revealed an apparently normal female karyotype (46,XX) (Supporting Information Figure S1). The remaining family members were healthy. We enrolled three unaffected family members (the proband's father [II 1], mother [II 2], and her younger brother [III 1]) and 11 unrelated healthy individuals as control subjects, and collected their peripheral blood samples for subsequent analysis. The study was approved by the Ethics Committee of Peking University School and Hospital of Stomatology (PKUSSIRB-2016113122). Written informed consent was provided by all participants and/or their legal guardians.

2.2 | DNA extraction and gene sequencing

Genomic DNA was extracted using a TIANamp Blood DNA mini kit (Tiangen, Beijing, China) according to the manufacturer's

instructions. Primers were designed using Primer3 (http://bioinfo. ut.ee/primer3-0.4.0/) to amplify the coding exons and intronic splice site junctions of the *PITX2A*, *PITX2B*, and *PITX2C* isoforms. Supporting Information Table S1 shows the primer sequences. The *PITX2* gene was amplified by PCR using TaKaRa Ex Taq (Takara Bio, Kyoto, Japan), and the products were purified and sequenced using an ABI 377 Automatic Sequencer (Applied Biosystems, Foster City, CA, USA). All DNA sequences were analyzed using Mutation Surveyor (SoftGenetics, State College, PA, USA).

2.3 | qPCR

DNA quantitative PCR was carried out in triplicate for *PITX2* and its neighboring genes using the ABI Prism 7500 Real-Time PCR System (Applied Biosystems) and SYBR Green Master Mix (Roche Diagnostics, Indianapolis, IN, USA). Primers for qPCR were designed using Primer3. The primer sequences and positions of each primer at chromosome 4 are summarized in Supporting Information Table S2.

The optimized primer concentrations for amplification of each amplicon were determined to ensure that the efficiencies were similar between the target and reference genes and approximately equaled 1. The efficiency of each primer set was determined using standard curve analysis, and twofold serially diluted normal control DNA samples were used to generate the curves. The method propose by Grimholt, Urdal, Klingenberg, and Piehler (2014) was used to determine whether two amplifications had the same efficiency (Grimholt et al., 2014), and the optimized DNA template concentration for each amplification was determined empirically.

All samples were prepared with the same master mix and run in triplicate in a final reaction volume of 20 μl. Each well contained 5 ng of DNA, 0.2–0.9 μM of each locus-specific primer pair for the target reference gene, 2× SYBR Green PCR Master Mix, and pure water for high-pressure liquid chromatography. The thermal cycling conditions were a prerun of 2 min at 50°C and 10 min at 95°C, followed by 40 cycles at 95°C for 15 s and 60°C for 1 min. The amplified products were routinely analyzed using melting curve analysis to exclude amplifications containing nonspecific products or primer dimers. Experiments were performed at least two times.

The fluorescence emission from each sample was analyzed using Sequence Detection System software (SDS version 2.3; Applied Biosystems). The relative gene expression was measured by subtracting the C_t values of the target (SEC24B, ENPEP, PITX2-8, PITX2-1, and ALPK1) from those of the control (GAPDH) gene of the RS samples and those of the control samples using the $2^{-\Delta\Delta C_t}$ method (Livak & Schmittgen, 2001).

2.4 | CMA

The CytoScan HD array platform (Affymetrix, Santa Clara, CA, USA) was applied to validate the deletions and determine the exact genomic location of the deleted regions. The entire procedure was
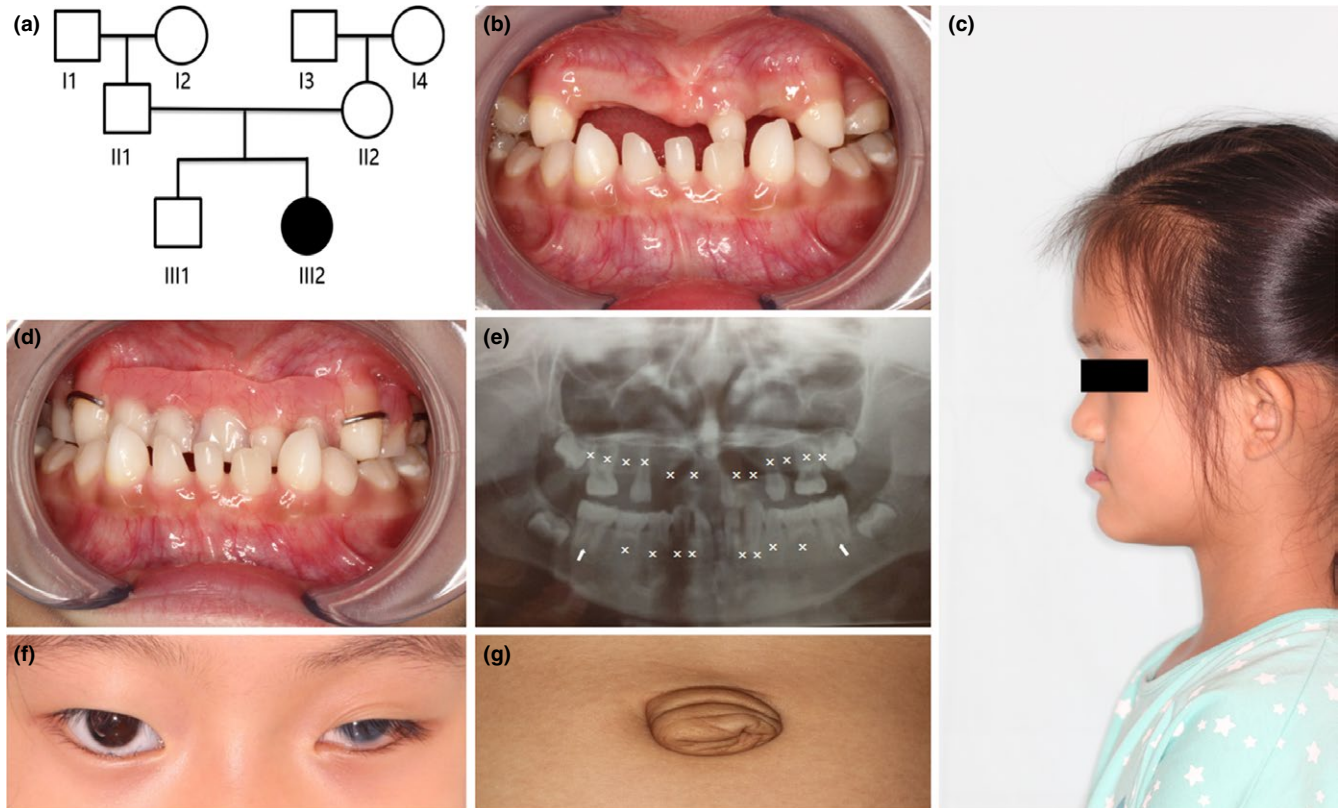
FIGURE 1 The pedigree of the family and clinical features of the patient. (a) Pedigree of the family of the patient with RS. (b) Intraoral view of the patient. (c) Lateral facial image of the patient. (d) Intraoral view of the patient with a simple removable acrylic prosthesis. (e) A pantomographic radiograph of the patient. Crosses indicate the lack of permanent teeth, while arrows indicate taurodontism. (f) The ocular features of the patient's left eye. (g) Protuberant umbilicus in the patient [Colour figure can be viewed at wileyonlinelibrary.com]

performed according to the manufacturer's instructions. DNA (at least 250 ng) was extracted using the above-mentioned method.

Raw data collected from the CMA were analyzed using Affymetrix Chromosome Analysis Suite (ChAS) software, and the output data were interpreted according to the 2010 guidelines of the American College of Medical Genetics and Genomics with the help of the Database of Genomic Variants (http://dgv.tcag.ca/dgv/app/home) and the Online Mendelian Inheritance in Man database (OMIM; http://www.omim.org).

3 | RESULTS

3.1 | Clinical findings

The proband, a 7-year-old girl, was the only member affected by RS in this nonconsanguineous Chinese family (Figure 1a). Intraoral examination revealed severe hypodontia and conical teeth (Figure 1b). She had a midface deficiency, and her forehead was prominent (Figure 1c). The patient was provided a removable acrylic partial denture for managing her immediate aesthetic needs (Figure 1d). A pantomographic radiograph obtained to determine the pattern of hypodontia showed severe hypodontia that affected the maxillary and mandibular incisors and premolars among the permanent teeth along with taurodontism (Figure 1e).

The patient's maxillary labial frenum was hyperplastic, and a reverse overjet and class III molar relationship were also noted. She presented with polycoria, corectopia, and corneal defect in her left eye (Figure 1f). She had undergone a trabeculectomy when she was 8 months old. Redundant periumbilical skin was also noted (Figure 1g). Intraoral images for the patient's parents are provided as Supporting Information Figure S2.

3.2 | Mutation results

No sequence variations were detected in the coding regions or exon–intron junctions of the *PITX2* gene. However, although some SNPs in the relative control were heterozygotic, the proband was consistently homozygotic (Figure 2). The odd distribution of the genotype of the SNPs in the noncoding regions of the entire family suggested the presence of a deletion of the *PITX2* gene (Table 1).

3.3 | CNV analysis

The slope coefficients of the standard curves of the six reactions (*GAPDH*, *SEC24B*, *ENPEP*, *PITX2-8*, *PITX2-1*, and *ALPK1*) ranged from 3.2 to 3.4, indicating a PCR amplification efficiency exceeding 95%. The r^2 values for the propagation of *GAPDH*, *SEC24B*, *ENPEP*,
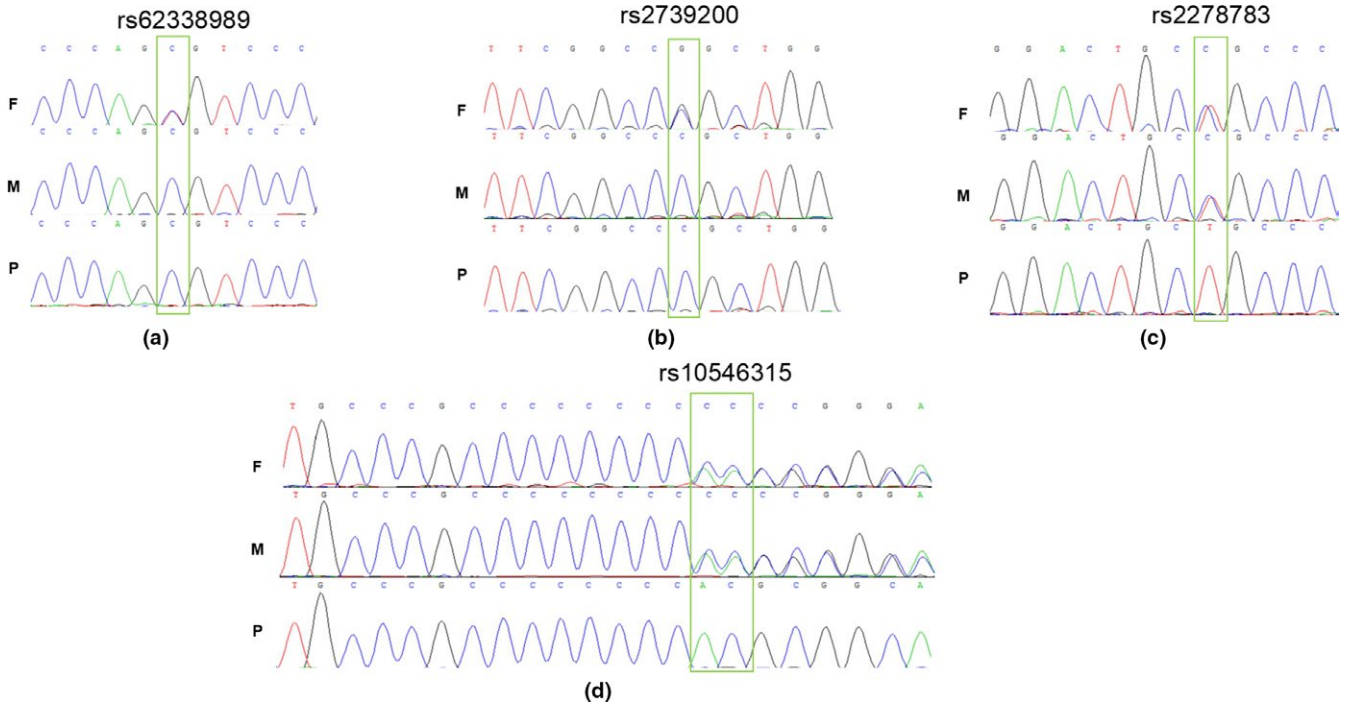
FIGURE 2 Sequences with SNPs found in this family. (a) rs62338989, (b) rs2739200, (c) rs2278783, (d) rs10546315. F: proband's father; M: proband's mother; P: proband (daughter) [Colour figure can be viewed at wileyonlinelibrary.com]

	rs62338989	rs2739200	rs10546315	rs2278783
Father	C/T	C/G	--/-G	C/T
Mother	C/C	C/C	--/-G	C/T
Proband (daughter)	C/C	C/C	--/--	T/T
P*	1/2	1/2	1/4	1/4

TABLE 1 The genotype of SNPs found in this family

Notes. P*: The probability of the proband being homozygous for each SNP. The probability of the proband always being homozygous for these four SNPs was 1/64 (1/2*1/2*1/4*1/4).
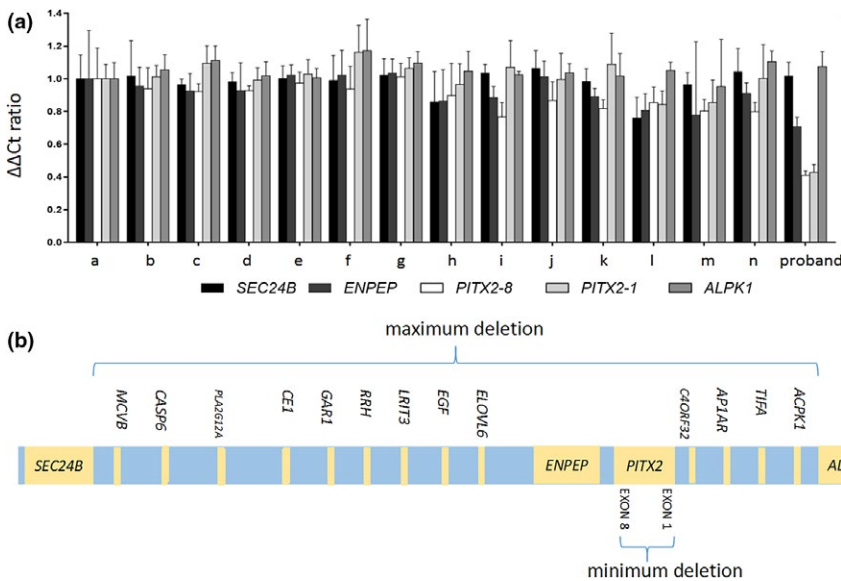
FIGURE 3 Copy number analysis conducted using qPCR. (a) Real-time quantitative PCR assay with five locus-specific primers designed for detection of chromosome 4q25 deletion in 14 normal controls and the proband. $\Delta\Delta C_t$ ratios of about 1.0 indicate a diploid genome, while $\Delta\Delta C_t$ ratios of about 0.5 indicate a deletion. (b) The size of the chromosome 4q25 deletion detected in the family of the proband with RS, with its minimal and maximal boundaries. The genes within this deletion are depicted (not to scale) [Colour figure can be viewed at wileyonlinelibrary.com]

PITX2-8, *PITX2-1*, and *ALPK1* DNA all exceeded 0.99. The log DNA dilution was plotted vs ΔC_t ($C_{t, Target} - C_{t, GAPDH}$). The absolute values of the slope were all <0.1, indicating that the efficiencies of the target and reference genes were similar. Thus, valid $2^{-\Delta\Delta C_t}$ calculation was ensured.

Genomic quantitative PCR was used to quantify deletions involving *PITX2* and its neighboring genes. A deletion involving *PITX2* was identified in the proband (Figure 3). The qPCR amplicon for *ALPK1* was 1,643,336 bp away from *PITX2* exon 1 (*PITX2-1*). As *PITX2-1* was deleted in the patient but ALPK1 was not, it appears that one deletion breakpoint lies between *PITX2-1* and *ALPK1*. In the same way, the qPCR amplicon for *SEC24B* was 1,155,558 bp away from *PITX2* exon 8 (*PITX2-8*), and as *PITX2-8* but not *SEC24B* was deleted in our patient, the other breakpoint of the deletion seems to be located between these two amplicons. Thus, the maximum size of the deletion was estimated to be 2,822,464 bp, including the following 15 genes: *MCVB*, *CASP6*, *PLA2G12A*, *CE1*, *GAR1*, *RRH*, *LRIT3*, *EGF*, *ELOVL6*, *ENPEP*, *PITX2*, *C4ORF32*, *AP1AR*, *TIFA*, and *ACPK1*. The minimum size of the deletion was estimated at 23,570 bp, to include only the *PITX2* gene.

The hemizygous deletion was confirmed by CMA, and the precise size of the deletion determined by CMA was 0.47 Mb (chr4: 111, 334, 313–111, 799, 327, GRCh37/hg19) including two genes, namely *PITX2* and *ENPEP* (Figure 4). In addition, a 0.86-Mb deletion (chr2: 110, 504, 318–111, 365, 996, GRCh37/hg19) including 16 genes from *RGPD5* to *LOC151009* and a 0.7-Mb duplication (chr14: 106, 246, 785–106, 948, 691, GRCh37/hg19) including no genes were also found in chromosomes 2 and 14, respectively. Six copy-neutral losses of heterozygosity were also detected in this patient.

4 | DISCUSSION

In the present study, we reported a novel deletion involving *PITX2* and *ENPEP* in a Chinese patient with RS. To date, about 11 microscopic deletions including *PITX2* have been reported in relation to RS, accounting for 13% of all patients with this condition (D'Haene et al., 2011; de la Houssaye et al., 2006; Engenheiro et al., 2007; Lines et al., 2004; Seifi et al., 2016; Titheradge et al., 2014). To our knowledge, our study represents the first case of RS caused by CNV of the *PITX2* gene in a proband of Chinese pedigree.

The dental phenotypes of RS include hypodontia, microdontia, conical teeth, hypoplasia of the enamel, and taurodontism (Waldron et al., 2010). The link between *PITX2* and tooth development was identified for the first time in patients with RS (Semina et al., 1996).
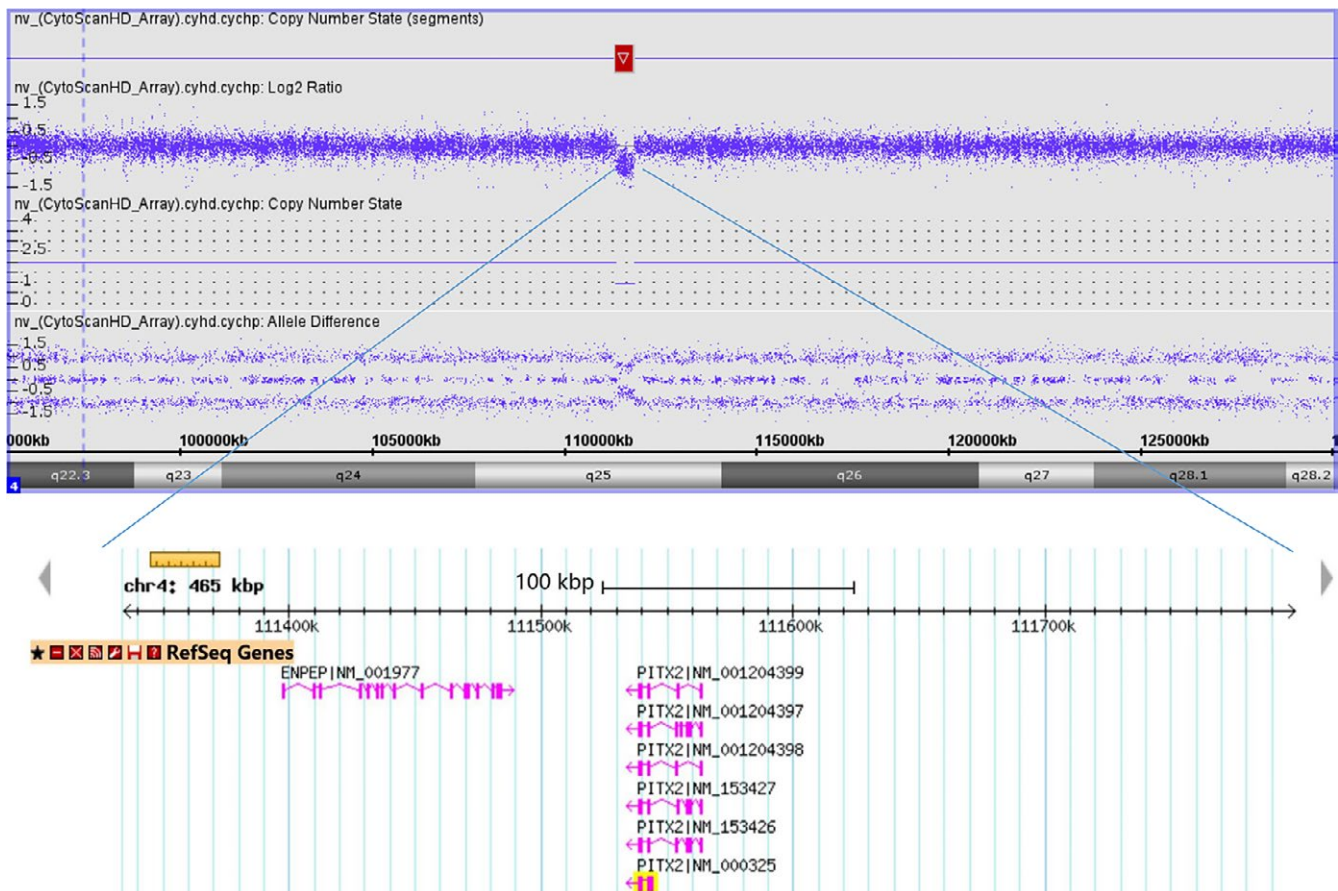
FIGURE 4 Copy number analysis conducted using CMA. An approximately 0.47-Mb (chr4: 111, 334, 313–111, 799, 327, GRCh37/hg19) deletion including two genes (*PITX2* and *ENPEP*) was identified [Colour figure can be viewed at wileyonlinelibrary.com]
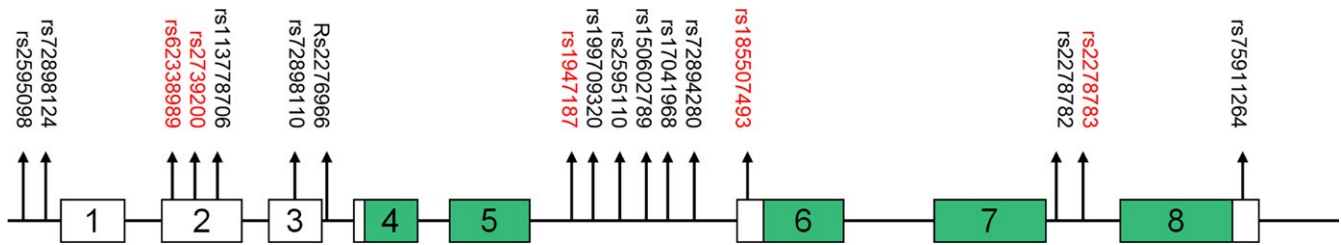
FIGURE 5 Positions of tag SNPs in PITX2 [Colour figure can be viewed at wileyonlinelibrary.com]

Lin et al. (1999) reported that tooth development is arrested at the invagination/bud stage in *PITX2*-knockout mice(Lin et al., 1999). PITX2 is one of the earliest epithelial markers of tooth development and is considered to be the main regulator of transcriptional hierarchy in early tooth development (Tucker & Sharpe, 2004). Many signaling molecules and transcription factors, such as FGF8, BMP4, and DLX2, that contribute to the large network of gene regulation in tooth and craniofacial development are related to PITX2 (Green et al., 2001; Li et al., 2014; Lin et al., 2007; Liu et al., 2003; St et al., 2000). FGF8 and BMP4 act as morphogenetic signals and mediate inductive interactions during tooth and craniofacial development. FGF8 failed to be expressed in *PITX2*-null embryos, and FGF8-socked beads can maintain or induce the expression of PITX2 (Lu, Pressman, Dyer, Johnson, & Martin, 1999; St et al., 2000). A positive feedback loop between PITX2 and FGF8 exists in the developing mandible (St et al., 2000). A study analyzing different *PITX2* allelic combinations encoding different levels of PITX2 demonstrated that maintenance of FGF8 expression requires low level of PITX2(Liu et al., 2003). In contrast, the developing mandible has a negative feedback loop between PITX2 and BMP4, and high PITX2 expression is needed to repress BMP signaling (Liu et al., 2003; St et al., 2000). Moreover, a PITX2 binding site in the *BMP4* enhancer was identified (Jumlongras et al., 2012). However, the exact molecular associations among these genes and the relationship between genes and phenotypes remain to be elucidated.

Paired-like homeodomain 2 mutations can cause RS as well as some mild ARS cases and non-ARS anterior segment dysgenesis, such as RA, AR, or Peters' anomaly (Reis et al., 2012; Tumer & Bach-Holm, 2009). However, almost all cases of ARS caused by *PITX2* deletions are RS, which is the most severe form of ARS (for more detailed information, see Supporting Information Table S3). A study suggested that differences in the clinical severity of ARS may be directly related to the function of the mutant PITX2 proteins (Kozlowski & Walter, 2000). For example, PITX2 R84W, a mutant causing ARS of low phenotypic severity (without tooth anomalies), can transactivate the *DLX2* promoter similar to wide-type PITX2. In contrast, PITX2 T68P, a mutation causing RS with tooth anomalies, cannot do this (Espinoza, Cox, Semina, & Amendt, 2002). DLX2 expression is required for tooth and craniofacial development, and the *DLX2* promotor is the natural target of PITX2. The difference between these two mutants in terms of DNA binding and transactivating the *DLX2* promotor may underlie their clinical differences. However, in patients with *PITX2* deletions, 50%

of the function is lost, so the phenotypic abnormalities in these patients are severe.

Previous studies have found that patients with gene microdeletions including *PITX2* had some phenotypes that do not occur in patients with classic RS, such as short stature and learning or behavioral difficulties (Lines et al., 2004; Titheradge et al., 2014). However, the patient in our study, who had gene microdeletions, did not show these non-RS symptoms. The genes included in the deleted region may have contributed to this difference. Titheradge et al. (2014) reported four patients with deletions that overlapped *PITX2* at 4q25 and observed that three of them had learning difficulties (Titheradge et al., 2014). On comparing the contiguous genes of the deletion regions, they found that the patient with no learning difficulties had the smallest microdeletion, including only *PITX2*, *ENPEP*, and two other pseudogenes, while the other three patients had a deletion region encompassing more contiguous genes. Through genotype–phenotype correlation, *NEUROG2*, *UGT8*, *NDST3*, and *PRSS12* were proposed as candidate genes responsible for cognitive impairment and congenital anomalies (Titheradge et al., 2014). In the present study, the deletion region was comparatively small (encompassing only *PITX2* and *ENPEP*) and did not include these five neuronal genes, which could explain why our patient had no learning difficulties. Thus, the exact mapping of deletions and detailed phenotyping in patients with microdeletions will elucidate the role of genes in the deletion region. The clinical comparison of cases with fine-mapped gene deletion including *PITX2* is shown in Supporting Information Table S3.

Using Sanger sequencing, we found no mutations in the *PITX2* coding area, but the distribution of the SNP genotype among the patient's family members provided clues about the deletion of *PITX2* gene. Irrespective of what the genotype of the parents was, the genotype of the proband was homozygotic. This state of homozygosity has two interpretations. The first is that the bases of the two chromosomes in the same location are always the same. The other explanation is that the gene region including these locations is deleted. The probability of the former hypothesis is 1/64 (Table 1), which is very small. Therefore, we assumed that the proband might have a gene deletion including these SNP loci.

We selected some tag SNPs for SNP analysis of *PITX2* to further support this hypothesis. Supporting Information Figure S3 shows the process of screening tag SNPs. There were 17 tag SNPs in total after our screening process. The information of these SNPs is shown in Supporting Information Table S4 and Figure 5. They were all in the

specific region of *PITX2* (exons, exon–intron boundaries, or promoters). And the genotypes of them could be simultaneously obtained by Sanger sequencing while screening *PITX2* gene mutations. These tag SNPs could be used to screen *PITX2* gene deletion preliminarily by other researchers. The distribution of tag SNPs genotypes in this family also proved the validity of SNP analysis for prescreening gene deletion (for detailed information, see Supporting Information Table S5).

In summary, we suspected and detected *PITX2* gene deletion in a patient of Chinese pedigree with RS using SNP analysis and qPCR, and we used CMA to ascertain the exact size of the deletion. Our study suggests an important role of *PITX2* in RS and highlights the necessity to detect CNVs in patient with RS without mutations in *PITX2*.

ACKNOWLEDGEMENTS

CONFLICT OF INTEREST

None to declare.

AUTHOR CONTRIBUTIONS

Y. Yang contributed to the research design, contributed to the acquisition, analyzed the data, and drafted the manuscript. X. Wang contributed to the acquisition, analyzed the data, and drafted the manuscript. Y. Zhao contributed to the analysis of data and revised the manuscript critically. M. Qin contributed to the research design, analyzed the data, and revised the manuscript critically.

ORCID

Yi Yang http://orcid.org/0000-0003-0173-7306

REFERENCES

Cella, W., de Vasconcellos, J. P., de Melo, M. B., Kneipp, B., Costa, F. F., Longui, C. A., & Costa, V. P. (2006). Structural assessment of PITX2, FOXC1, CYP1B1, and GJA1 genes in patients with Axenfeld-Rieger syndrome with developmental glaucoma. *Investigative Ophthalmology & Visual Science*, 47, 1803–1809. https://doi.org/10.1167/iovs.05-0979

Childers, N. K., & Wright, J. T. (1986). Dental and craniofacial anomalies of Axenfeld-Rieger syndrome. *Journal of Oral Pathology*, 15, 534–539. https://doi.org/10.1111/j.1600-0714.1986.tb00572.x

de la Houssaye, G., Bieche, I., Roche, O., Vieira, V., Laurendeau, I., Arbogast, L., … Abitbol, M. (2006). Identification of the first intragenic deletion of the PITX2 gene causing an Axenfeld-Rieger Syndrome: Case report. *BMC Medical Genetics*, 7, 82. https://doi.org/10.1186/1471-2350-7-82

D'Haene, B., Meire, F., Claerhout, I., Kroes, H. Y., Plomp, A., Arens, Y. H., … De Baere, E. (2011). Expanding the spectrum of FOXC1 and PITX2 mutations and copy number changes in patients with anterior segment malformations. *Investigative Ophthalmology & Visual Science*, 52, 324–333. https://doi.org/10.1167/iovs.10-5309

Dressler, S., Meyer-Marcotty, P., Weisschuh, N., Jablonski-Momeni, A., Pieper, K., Gramer, G., & Gramer, E. (2010). Dental and craniofacial anomalies associated with axenfeld-rieger syndrome with PITX2 mutation. *Case Reports in Medicine*, 2010, 621984.

Engenheiro, E., Saraiva, J., Carreira, I., Ramos, L., Ropers, H. H., Silva, E., … Tumer, Z. (2007). Cytogenetically invisible microdeletions involving PITX2 in Rieger syndrome. *Clinical Genetics*, 72, 464–470. https://doi.org/10.1111/j.1399-0004.2007.00879.x

Espinoza, H. M., Cox, C. J., Semina, E. V., & Amendt, B. A. (2002). A molecular basis for differential developmental anomalies in Axenfeld-Rieger syndrome. *Human Molecular Genetics*, 11, 743–753. https://doi.org/10.1093/hmg/11.7.743

Green, P. D., Hjalt, T. A., Kirk, D. E., Sutherland, L. B., Thomas, B. L., Sharpe, P. T., … Amendt, B. A. (2001). Antagonistic regulation of Dlx2 expression by PITX2 and Msx2: Implications for tooth development. *Gene Expression*, 9, 265–281. https://doi.org/10.3727/000000001783992515

Grimholt, R. M., Urdal, P., Klingenberg, O., & Piehler, A. P. (2014). Rapid and reliable detection of alpha-globin copy number variations by quantitative real-time PCR. *BMC Hematology*, 14, 4. https://doi.org/10.1186/2052-1839-14-4

Hjalt, T. A., & Semina, E. V. (2005). Current molecular understanding of Axenfeld-Rieger syndrome. *Expert Reviews in Molecular Medicine*, 7, 1–17.

Jumlongras, D., Lachke, S. A., O'Connell, D. J., Aboukhalil, A., Li, X., Choe, S. E., … Maas, R. L. (2012). An evolutionarily conserved enhancer regulates Bmp4 expression in developing incisor and limb bud. *PLoS ONE*, 7, e38568. https://doi.org/10.1371/journal.pone.0038568

Kozlowski, K., & Walter, M. A. (2000). Variation in residual PITX2 activity underlies the phenotypic spectrum of anterior segment developmental disorders. *Human Molecular Genetics*, 9, 2131–2139. https://doi.org/10.1093/hmg/9.14.2131

Li, X., Venugopalan, S. R., Cao, H., Pinho, F. O., Paine, M. L., Snead, M. L., … Amendt, B. A. (2014). A model for the molecular underpinnings of tooth defects in Axenfeld-Rieger syndrome. *Human Molecular Genetics*, 23, 194–208. https://doi.org/10.1093/hmg/ddt411

Lin, D., Huang, Y., He, F., Gu, S., Zhang, G., Chen, Y., & Zhang, Y. (2007). Expression survey of genes critical for tooth development in the human embryonic tooth germ. *Developmental Dynamics*, 236, 1307–1312. https://doi.org/10.1002/(ISSN)1097-0177

Lin, C. R., Kioussi, C., O'Connell, S., Briata, P., Szeto, D., Liu, F., … Rosenfeld, M. G. (1999). Pitx2 regulates lung asymmetry, cardiac positioning and pituitary and tooth morphogenesis. *Nature*, 401, 279–282. https://doi.org/10.1038/45803

Lines, M. A., Kozlowski, K., Kulak, S. C., Allingham, R. R., Heon, E., Ritch, R., … Walter, M. A. (2004). Characterization and prevalence of PITX2 microdeletions and mutations in Axenfeld-Rieger malformations. *Investigative Ophthalmology & Visual Science*, 45, 828–833. https://doi.org/10.1167/iovs.03-0309

Liu, W., Selever, J., Lu, M. F., & Martin, J. F. (2003). Genetic dissection of Pitx2 in craniofacial development uncovers new functions in branchial arch morphogenesis, late aspects of tooth morphogenesis and cell migration. *Development*, 130, 6375–6385. https://doi.org/10.1242/dev.00849

Livak, K. J., & Schmittgen, T. D. (2001). Analysis of relative gene expression data using real-time quantitative PCR and the 2(T)(-Delta Delta C) method. *Methods*, 25, 402–408. https://doi.org/10.1006/meth.2001.1262

Lu, M. F., Pressman, C., Dyer, R., Johnson, R. L., & Martin, J. F. (1999). Function of Rieger syndrome gene in left-right asymmetry and craniofacial development. *Nature*, 401, 276–278. https://doi.org/10.1038/45797

Micheal, S., Siddiqui, S. N., Zafar, S. N., Venselaar, H., Qamar, R., Khan, M. I., & den Hollander, A. I. (2016). Whole exome sequencing identifies a heterozygous missense variant in the PRDM5 gene in a family with Axenfeld-Rieger syndrome. *Neurogenetics*, 17, 17–23. https://doi.org/10.1007/s10048-015-0462-0

Phillips, J. C., Del, B. E. A., Haines, J. L., Pralea, A. M., Cohen, J. S., Greff, L. J., & Wiggs, J. L. (1996). A second locus for Rieger syndrome maps to chromosome 13q14. *American Journal of Human Genetics*, 59, 613–619.

Reis, L. M., Tyler, R. C., Volkmann Kloss, B. A., Schilter, K. F., Levin, A. V., Lowry, R. B., ... Semina, E. V. (2012). PITX2 and FOXC1 spectrum of mutations in ocular syndromes. *European Journal of Human Genetics*, 20, 1224–1233. https://doi.org/10.1038/ejhg.2012.80

Seifi, M., Footz, T., Taylor, S. A., Elhady, G. M., Abdalla, E. M., & Walter, M. A. (2016). Novel PITX2 gene mutations in patients with Axenfeld-Rieger syndrome. *Acta Ophthalmologica*, 94, e571–e579. https://doi.org/10.1111/aos.13030

Seifi, M., & Walter, M. A. (2017). Axenfeld-Rieger syndrome. *Clinical Genetics*, 93, 1123–1130.

Semina, E. V., Reiter, R., Leysens, N. J., Alward, W. L., Small, K. W., Datson, N. A., ... Murray, J. C. (1996). Cloning and characterization of a novel bicoid-related homeobox transcription factor gene, RIEG, involved in Rieger syndrome. *Nature Genetics*, 14, 392–399. https://doi.org/10.1038/ng1296-392

St, A. T. R., Zhang, Y., Semina, E. V., Zhao, X., Hu, Y., Nguyen, L., ... Chen, Y. (2000). Antagonistic signals between BMP4 and FGF8 define the expression of Pitx1 and Pitx2 in mouse tooth-forming anlage. *Developmental Biology*, 217, 323–332.

Titheradge, H., Togneri, F., McMullan, D., Brueton, L., Lim, D., & Williams, D. (2014). Axenfeld-Rieger syndrome: Further clinical and array delineation of four unrelated patients with a 4q25 microdeletion. *American Journal of Medical Genetics. Part A*, 164A, 1695–1701. https://doi.org/10.1002/ajmg.a.36540

Tucker, A., & Sharpe, P. (2004). The cutting-edge of mammalian development; how the embryo makes teeth. *Nature Reviews Genetics*, 5, 499–508. https://doi.org/10.1038/nrg1380

Tumer, Z., & Bach-Holm, D. (2009). Axenfeld-Rieger syndrome and spectrum of PITX2 and FOXC1 mutations. *European Journal of Human Genetics*, 17, 1527–1539. https://doi.org/10.1038/ejhg.2009.93

Waldron, J. M., McNamara, C., Hewson, A. R., & McNamara, C. M. (2010). Axenfeld-Rieger syndrome (ARS): A review and case report. *Special Care in Dentistry*, 30, 218–222. https://doi.org/10.1111/j.1754-4505.2010.00153.x

SUPPORTING INFORMATION

Additional supporting information may be found online in the Supporting Information section at the end of the article.